Emergence of cooperatively reorganizing cluster and super-Arrhenius dynamics of fragile supercooled liquids

Ankit Singh [1], Sarika Maitra Bhattacharyya [2], and Yashwant Singh [1]
[1]*Department of Physics, Banaras Hindu University, Varanasi 221 005, India*
[2]*Polymer Science and Engineering Division, CSIR-National Chemical Laboratory, Pune 411008, India*

(Received 12 November 2020; accepted 12 March 2021; published 29 March 2021)

In this paper, we develop a theory to calculate the structural relaxation time τ_α of fragile supercooled liquids. Using the information of the configurational entropy and structure, we calculate the number of dynamically free, metastable, and stable neighbors around a central particle. In supercooled liquids, the cooperatively reorganizing clusters (CRCs) in which the stable neighbors form "stable" nonchemical bonds with the central particle emerge. For an event of relaxation to take place, these bonds have to reorganize irreversibly; the energy involved in the processes is the effective activation energy of relaxation. The theory brings forth a temperature T_a and a temperature-dependent parameter $\psi(T)$ which characterize slowing down of dynamics on cooling. It is shown that the value of $\psi(T)$ is equal to 1 for $T > T_a$, indicating that the underlying microscopic mechanism of relaxation is dominated by the entropy-driven processes, while for $T < T_a$, $\psi(T)$ decreases on cooling, indicating the emergence of the energy-driven processes. This crossover of $\psi(T)$ from high to low temperatures explains the crossover seen in τ_α. The dynamics of systems that may have similar static structure but very different dynamics can be understood in terms of $\psi(T)$. We present results for the Kob-Anderson model for three densities and show that the calculated values of τ_α are in excellent agreement with simulation values for all densities. We also show that when $\psi(T)$, τ_α, and other quantities are plotted as a function of T/T_a (or T_a/T), the data collapse on master curves.

DOI: 10.1103/PhysRevE.103.032611

I. INTRODUCTION

When a liquid is supercooled, bypassing its crystallization, it continues to remain structurally disordered, but its dynamics slows down so quickly that below a temperature, called the glass temperature T_g, the structural relaxation takes such a long time that it becomes almost impossible to observe [1]. The structural relaxation time, τ_α, represents the time required for the liquid to return to equilibrium after a small perturbation. The super-Arrhenius temperature dependence of τ_α (or the viscosity) is the defining characteristic of a "fragile" liquid [2,3]. The super-Arrhenius behavior suggests that the effective activation energy for the relaxation in a fragile liquid increases with decreasing temperature. The underlying reason for such a behavior is understood in terms of increasing the cooperativity of relaxation on cooling. The cooperativity can be defined in terms of number of particles which move in some sort of concert in order for an elementary relaxation event to occur. These particles may be distributed in a region without forming a compact structure and share the space with other particles [4,5]. In such a situation, it would not be possible to characterize cooperativity in terms of a spatial length. Alternatively, one can think of a compact cooperative region defined by a length ξ; the number of particles in the region varies as ξ^d, where d is spatial dimension [6,7]. To have a precise picture of cooperativity (or the cooperative region), its determination as a function of temperature and calculation of the effective activation energy from microscopic interactions between particles have been the major focus of the theoretical description of supercooled liquids and the glass transition [6–23].

Is there any local structural order in a liquid that grows rapidly on cooling and can be associated with the cooperativity? This question has been the subject of much activity of the past several years [12–23], as its resolution would lead to a better understanding of glassy phenomena and would provide insights into the underlying microscopic mechanism of the relaxation. However, liquid structure determined from scattering experiments that give information at the level of two-point correlation functions, such as the structure factor and the pair correlation function shows no such local order. This led to the conclusion that if at all there is any local order linked to the cooperativity, it would have to be very subtle and hidden to the pair correlation function. This spurred several proposals of local preferred structure such as the "point-to-set length" [17–20] and the "patch correlation length" [21–23] with varying success. The main difficulty is that one does not know how to distinguish an amorphous ordered structure from the one that exists in a normal liquid [8].

In the Adam and Gibbs theory [6] as well as in the random first-order transition (also known as the mosaic) theory [7,24,25], the cooperative region is expressed in terms of the configurational entropy. Adam and Gibbs visualized a supercooled liquid as progressively organizing in larger cooperative regions that have to collectively reorganize and proposed that the number of particles in a "cooperatively rearranging

region (CRR)" is inversely proportional to the configurational entropy S_c. Since the configurational entropy $S_c(T)$ decreases on lowering the temperature, the number of particles in the cooperative region increases. The relaxation time τ_α is the time needed to rearrange the region and is given by

$$\tau_\alpha = \tau_0 \exp\left[\frac{A}{TS_c(T)}\right], \tag{1.1}$$

where A is a temperature-independent phenomenological parameter and τ_0 is the microscopic timescale.

On the other hand, the mosaic theory assumes nucleation of so-called "entropic droplets" between different metastable configurations that makes the supercooled liquid as a patchwork of local metastable configurations. A static length ξ in terms of which the size of the droplet is expressed is shown to be $\xi = (Y(T)/TS_c)^{\frac{1}{d-\theta}}$, where d is the spatial dimension, θ is an exponent related to the interface energy, and $Y(T)$ is the surface tension [24,25]. The relaxation time is related to the configurational entropy by the relation

$$\tau_\alpha = \tau_0 \exp\left[\frac{1}{T}\left(\frac{Y(T)}{TS_c(T)}\right)^{\phi}\right], \tag{1.2}$$

where $\phi = \frac{d}{d-\theta}$. In order to find values of $\xi(T)$ and $\tau_\alpha(T)$, one has to know values of $Y(T)$ and θ.

It has recently been shown [26] that in a supercooled (supercompressed) liquid some particles get localized in potential wells and form long-lived (stable) nonchemical bonds between them. A cluster of these bonded particles collectively rearranges and creates an effective potential energy barrier for relaxation. The number of particles in the cluster is calculated from the data of pair correlation function. In this paper, we extend the theory and report results for a glass-forming liquid.

The system we consider is the Kob-Anderson 80:20 mixture of Lennard-Jones particles consisting of two species of particles a and b [27]. All particles have the same mass m and the interaction between two particles of type $\alpha, \gamma \in [a, b]$ is given by

$$u_{\alpha\gamma}(r) = 4\epsilon_{\alpha\gamma}\left[\left(\frac{\sigma_{\alpha\gamma}}{r}\right)^{12} - \left(\frac{\sigma_{\alpha\gamma}}{r}\right)^{6}\right], \tag{1.3}$$

with $\epsilon_{aa} = 1$, $\sigma_{aa} = 1$, $\epsilon_{ab} = 1.5$, $\sigma_{ab} = 0.8$, $\epsilon_{bb} = 0.5$, and $\sigma_{bb} = 0.88$. Length, energy, and temperature are given in units of σ_{aa}, ϵ_{aa}, and ϵ_{aa}/k_B, respectively. The particle momenta of both species have identical Maxwell-Boltzmann distributions.

II. NUMBER OF "STABLE" AND "METASTABLE" BONDS FORMED BY A PARTICLE WITH ITS NEIGHBORS IN A LIQUID

In equilibrium, each particle of a liquid feels on the average similar potential energy barrier due to its interactions with neighbors, but its kinetic energy has a probability to have any value given by the Maxwell-Boltzmann distribution. Therefore, due to competition between the kinetic energy which makes particles move and the potential energy barrier that restricts particle motion, particles in a liquid acquire a wide range of dynamical states. It is intuitively clear that all those particles whose values of kinetic energy are high would be able to overcome the potential barrier and move around as free particles whereas all those particles whose values of kinetic energy are low would be trapped by the potential barrier. There are also particles whose values of kinetic energy are not high enough, but fluctuations embedded in the system may make them escape the barrier. We can therefore roughly divide particles into three groups of dynamical states: (i) free particles that move around and collide with other particles, (ii) particles that remain trapped (localized) and execute vibrational motions at well defined locations, and (iii) particles that are intermittent between trapped and free. The concentration of these particles depends on density and temperature, the potential energy barrier becomes higher on increasing the density and lowering the temperature, and the kinetic energy of particles decreases on decreasing the temperature. A supercooled liquid can therefore be considered as a network of particles connected with each other by (nonchemical) bonds with lifetimes varying from microscopic to macroscopic time. We now describe how to calculate the number of these particles from the data of radial distribution function.

A. Separation of $g(r)$ into parts representing particles of different dynamical states

The radial distribution function which for a simple liquid is defined as [28]

$$g(|\vec{r}_2 - \vec{r}_1|) \equiv g(r) = \frac{1}{N\rho}\langle \sum_{j}^{N}\sum_{j\neq k}^{N} \delta(\vec{r} - \vec{r}_j + \vec{r}_k)\rangle, \tag{2.1}$$

where N is number of particles, ρ is the number density, and the angular bracket denotes the ensemble average, tells us the probability of finding a particle at a distance r from a reference (central) particle. The average number of particles lying within the range r and $r + dr$ from the central particle in three dimensions is $4\pi\rho g(r) r^2 dr$. Since $g(r)$ defined by Eq. (2.1) has no information about particle momenta, one cannot say how many of these particles located in the region at a given time will remain there forever unless disturbed and how many of them will subsequently move away. To get such information, we define $g(r)$ of a binary mixture in the center-of-mass coordinates as [26]

$$g_{\alpha\gamma}(r) = \left(\frac{\beta}{2\pi\mu}\right)^{\frac{3}{2}} \int d\mathbf{p}\, e^{-\beta[\frac{p^2}{2\mu} + w_{\alpha\gamma}(r)]}, \tag{2.2}$$

where $\beta = (k_B T)^{-1}$ is the inverse temperature measured in units of the Boltzmann constant k_B and $\mathbf{p}$ is the relative momentum of a particle of mass $\mu = m/2$. The effective potential (potential of mean force) $w_{\alpha\gamma}(r) = -k_B T \ln g_{\alpha\gamma}(r)$ is sum of the (bare) pair potential energy $u_{\alpha\gamma}$ and the system-induced potential energy of interaction between a pair of particles of species α and γ separated by distance r [28]. The peaks and troughs of $g_{\alpha\gamma}(r)$ create, respectively, minima and maxima in $\beta w_{\alpha\gamma}(r)$ as shown in Fig. 1 for species a at $T = 0.45$ and $\rho = 1.20$. A region between two maxima, leveled as $i-1$ and i ($i \geqslant 1$), is denoted as ith shell and minimum of the shell as $\beta w_{\alpha\gamma}^{(id)}$. The value of ith maximum is denoted as $\beta w_{\alpha\gamma}^{(iu)}$ and its location is given by r_{ih}.

In a classical system, all those particles in region of ith shell whose energies are less or equal to $\beta w_{\alpha\gamma}^{(iu)}$, i.e.,

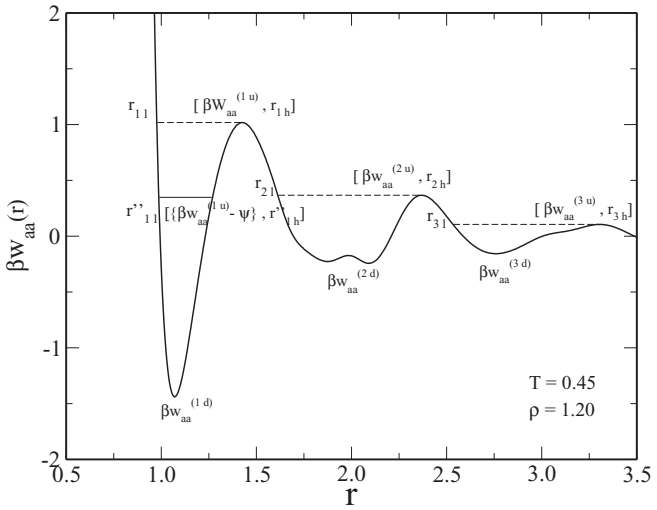

FIG. 1. The reduced effective potential $\beta w_{aa}(r)$ between a pair of particles of species α and γ separated by distance r (expressed in unit of σ_{aa}) in a system of Lennard-Jones at a density $\rho = 1.20$ and temperature $T = 0.45$. $\beta w_{aa}^{(iu)}, r_{ih}$ are, respectively, value and location of ith maximum and r_{il} is the location on the left-hand side of the shell where $\beta w_{aa}^{(i)}(r) = \beta w_{aa}^{(iu)}$ (shown by dashed line). The location r_{il}'' and r_{ih}'' are values of r on the left- and right-hand sides of the shell where $\beta w_{aa}^{(i)}(r) = [\beta w_{aa}^{(iu)} - \psi]$ (shown by full line). $\beta w_{aa}^{(id)}$ is the depth of the ith shell.

$\beta[\frac{p^2}{2\mu} + w_{\alpha\gamma}^{(i)}(r)] \leqslant \beta w_{\alpha\gamma}^{(iu)}$, will be trapped as they do not have enough energy to overcome the barrier $\beta w_{\alpha\gamma}^{(iu)}$. These particles can be considered to be bonded with the central particle. On the other hand, all those particles whose energies are higher than $\beta w_{\alpha\gamma}^{(iu)}$ or momenta higher than $\sqrt{2\mu w_{\alpha\gamma}^{(iu)}}$ are free to move around individually and collide with other particles as long as their momenta remain higher than the value mentioned above. When due to collisions a free particle loses its momentum and falls below $\sqrt{2\mu w_{\alpha\gamma}^{(iu)}}$, the particle gets trapped. At a given temperature and density, an equilibrium between free and bonded particles is established. The average number of these particles can be found from $g(r)$.

The averaged number of particles that form bonds with the central particle can be found from a part of $g_{\alpha\gamma}(r)$ defined as

$$g_{\alpha\gamma}^{(ib)}(r) = 4\pi\left(\frac{\beta}{2\pi\mu}\right)^{3/2} e^{-\beta w_{\alpha\gamma}^{(i)}(r)} \int_0^{\sqrt{2\mu[w_{\alpha\gamma}^{(iu)} - w_{\alpha\gamma}^{(i)}(r)]}} \times e^{-\beta p^2/2\mu} p^2 dp, \tag{2.3}$$

where $w_{\alpha\gamma}^{(i)}(r)$ is the effective potential in the range of $r_{il} \leqslant r \leqslant r_{ih}$ of ith shell. Here r_{il} is value of r where $w_{\alpha\gamma}^{(i)}(r) = w_{\alpha\gamma}^{(iu)}$ on the left-hand side of the shell (see Fig. 1. The number of particles in the shell which form bonds with the central particle of species α is

$$n_\alpha^{(b)} = 4\pi \sum_i \sum_\gamma \rho_\gamma \int_{r_{il}}^{r_{ih}} g_{\alpha\gamma}^{(ib)}(r) r^2 dr, \tag{2.4}$$

where summations are over all shells and over all species and ρ_γ is number density of γ species. This number $n_\alpha^{(b)}$ increases rapidly on lowering the temperature and increasing the density due to an increase in the number of shells surrounding the central particle and increase in values of maximum and minimum of each shell.

Since these bonded particles in each shell have a wide range of energies lying between maximum and minimum of the shell, they oscillate with a wide range of frequencies. However, all those particles whose energies are close to the maximum (barrier height) may not remain bonded for long due to fluctuations embedded in the system (bath) which drive them to escape the barrier. This is an entropy-driven process. In the case of an athermal system where only packing constraints matter, there are no energy parameters whatsoever; the bath drives all those particles of ith shell whose energies lie between $\beta w_{\alpha\gamma}^{(iu)} - 1$ and $\beta w_{\alpha\gamma}^{(iu)}$ out of the shell [26]. However, in a thermal system, the entropy-driven process is opposed by the energy-driven process; the system gains entropy but loses internal energy when particles escape the shell and the reverse happens when particles remain in the shell. This competition results in a diminishing bath role in driving particles out of shells. This led us to introduce a temperature-dependent parameter $\psi(T)$ ($\leqslant 1$) such that only those particles of ith shell whose energy lies between $\beta w_{\alpha\gamma}^{(iu)} - \psi$ and $\beta w_{\alpha\gamma}^{(iu)}$ are able to escape the shell. However, as is well known, the value of ψ in a normal (high-temperature) liquid is one. The departure from one is excepted to take place at lower temperatures where the role of energy parameters become important. In Sec. II B, we describe a method to determine its value.

The bonded particles can be divided into two groups, one that consists of particles that are able to escape from the shell and the ones which survive fluctuations and remain bonded unless disturbed. The first group of particles consists of all those particles whose energies lie between $[\beta w_{\alpha\gamma}^{(iu)} - \psi]$ and $\beta w_{\alpha\gamma}^{(iu)}$ and momenta between $\sqrt{2\mu[w_{\alpha\gamma}^{(iu)} - \psi k_B T - w_{\alpha\gamma}^{(i)}(r)]}$ and $\sqrt{2\mu[w_{\alpha\gamma}^{(iu)} - w_{\alpha\gamma}^{(i)}(r)]}$. These particles are called metastable particles and henceforth referred to as m particles. During the time they remain bonded, they oscillate in the shell with time periods depending upon their energies. It is obvious that trajectories of these particles are composed of a succession of periods of time when particles simply vibrate around well-defined locations (shells), separated by rapid jumps that are widely distributed in time. This feature has been observed in the computer simulation study of time-resolved square displacements of individual particles. The plateau observed at intermediate times in the mean-squared displacement is due to vibrations within shells.

The part of $g(r)$ that represents m particles in the ith shell can be written as

$$g_{\alpha\gamma}^{(im)}(r) = 4\pi\left(\frac{\beta}{2\pi\mu}\right)^{3/2} e^{-\beta w_{\alpha\gamma}^{(i)}(r)} \int_{\sqrt{2\mu[w_{\alpha\gamma}^{(iu)} - \psi k_B T - w_{\alpha\gamma}^{(i)}(r)]}}^{\sqrt{2\mu[w_{\alpha\gamma}^{(iu)} - w_{\alpha\gamma}^{(i)}(r)]}} \times e^{-\beta p^2/2\mu} p^2 dp, \tag{2.5}$$

Value of $g_{\alpha\gamma}^{(im)}(r)$ in a shell (see Fig. 5) starts from zero at $r = r_{il}'$ on the left-hand side and attains a maximum value at a value of r where $\beta w_{\alpha\gamma}^{(i)}(r)$ has its minimum value and then decreases and becomes zero at r_{ih}' on the right-hand side of the shell. The number of m particles around a particle of α species

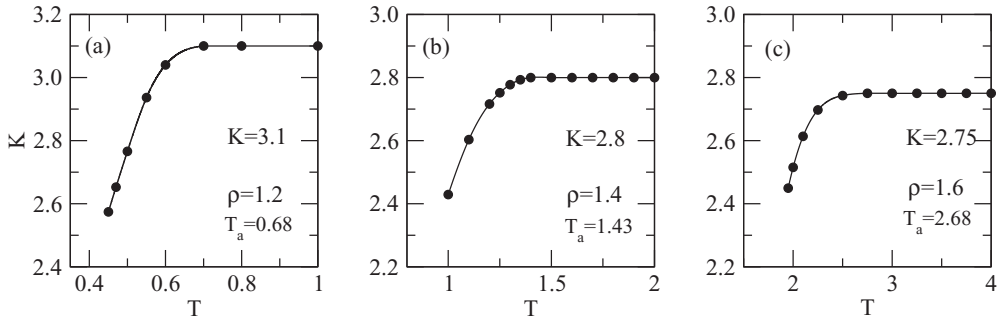

FIG. 2. Values of K as a function of temperature T found when $\psi = 1$ was taken in calculating values of number of s particles. The deviation of value of K from its constant value at low temperature is due to the fact that taking $\psi = 1$ at $T < T_a$ is not valid. Symbols represent calculated values and curves are least-square fit.

is found from $g_{\alpha\gamma}^{(im)}(r)$ using the relation

$$n_\alpha^{(m)} = 4\pi \sum_i \sum_\gamma \rho_\gamma \int_{r_{il}'}^{r_{ih}'} g_{\alpha\gamma}^{(im)}(r) r^2 dr. \tag{2.6}$$

A length scale which can be associated with a cluster of m particles formed around a central particle is equal to the range of $g_{\alpha\gamma}^{(m)}(r) \simeq g_{\alpha\gamma}(r) - 1$. This length increases upon lowering the temperature and increasing the density. The averaged number of m particles surrounding a central particle in a binary mixture is

$$n^{(m)} = x_a n_a^{(m)} + x_b n_b^{(m)}, \tag{2.7}$$

where x_α is the concentration of species α.

The second group of bonded particles are those whose energies are lower than $[\beta w_{\alpha\gamma}^{(iu)} - \psi]$ and particles whose momenta are lower than $\sqrt{2\mu[w_{\alpha\gamma}^{(iu)} - \psi k_B T - w_{\alpha\gamma}^{(i)}(r)]}$. These particles form stable bonds with the central particle and are referred to as s particles. The part of $g(r)$ that corresponds to these particles is

$$g_{\alpha\gamma}^{(is)}(r) = 4\pi \left(\frac{\beta}{2\pi\mu}\right)^{3/2} e^{-\beta w_{\alpha\gamma}^{(i)}(r)} \int_0^{\sqrt{2\mu[w_{\alpha\gamma}^{(iu)} - \psi k_B T - w_{\alpha\gamma}^{(i)}(r)]}} \times e^{-\beta p^2/2\mu} p^2 dp, \tag{2.8}$$

where $w_{\alpha\gamma}^{(i)}(r)$ is in the range $r_{il}'' \leqslant r \leqslant r_{ih}''$. Here r_{il}'' and r_{ih}'' are, respectively, value of r on the left- and the right-hand sides of the shell where $\beta w_{\alpha\gamma}^{(i)}(r) = \beta w_{\alpha\gamma}^{(iu)} - \psi$. The number of particles around an α particle is

$$n_\alpha^{(s)} = 4\pi \sum_i \sum_\gamma \rho_\gamma \int_{r_{il}''}^{r_{ih}''} g_{\alpha\gamma}^{(is)}(r) r^2 dr, \tag{2.9}$$

The averaged number of s-particles bonded with a central particle in a binary mixture is

$$n^{(s)} = x_a n_a^{(s)} + x_b n_b^{(s)}. \tag{2.10}$$

We have to know value of ψ as a function of T and ρ to calculate value of $n^{(s)}(T)$ and $n^{(m)}(T)$ in a given system.

B. Determination of temperature dependence of ψ and the number of particles in a cooperatively reorganizing cluster

We call the cluster formed by $n^{(s)}$, s particles bonded with the central particle as a cooperatively reorganizing cluster (CRC). For an event of structural relaxation to take place, the cluster has to reorganize irreversibly; the energy involved in this rearrangement is the energy with which the central particle is bonded with s particles. These particles are distributed in shells around the central particle where they share the region with other (mobile) particles. As the structure of the cluster is not compact, it cannot be measured in terms of spatial length. The CRC, therefore, differs from the Adam and Gibbs [6] "cooperatively rearranging region (CRR)," which is taken to be a compact structure [6,17]. We have more to say about this in Sec. V. The cooperativity here is defined in terms of number of bonds, $n^{(s)}$, formed by a particle with its neighbors. As the temperature is lowered, the number $n^{(s)}$ as well as the energy of each bond in the cluster would increase. As a consequence, the relaxation time growth with decreasing temperature is super-Arrhenius, i.e., faster than an exponential in inverse temperature.

Following Adam and Gibbs [6], we assume that the relation between the number of particles in a CRC and the configurational entropy can be written as

$$n^{(s)}(T) + 1 = \frac{K}{S_c(T)}, \tag{2.11}$$

where K is a temperature-independent constant and S_c is the configurational entropy per particle of the system. Values of S_c as function of temperature are found from relation $S_c(T) = S_{total}(T) - S_{vib}(T)$, where S_{total} is sum of the ideal gas entropy plus excess entropy arising due to interactions between particles and S_{vib} is the vibrational entropy arising due to short-time vibrational motions in a local potential energy minimum. Ingenious simulation techniques developed recently [29,30] have made it possible to find accurate values of S_c in supercooled region. In the present calculations, we use values of S_c reported in Ref. [31].

In order to determine the value of K, we first take $\psi = 1$ in Eqs. (2.8)–(2.10) and calculate $n^{(s)}(T)$ at different temperatures. Values of $n^{(s)}(T)$ are then used in Eq. (2.11) to calculate K. In Fig. 2, we plot K versus T at densities $\rho = 1.2$, 1.4, and 1.6. In all the cases, we find that K is constant above

TABLE I. Values of constant K, T_a, $T_{\rm onset}$, and T_{mc} at different densities.

ρ	K	T_a	$T_{\rm onset}$	T_{mc}
1.2	3.10	0.68	0.77	0.43
1.4	2.80	1.43	1.50	0.93
1.6	2.75	2.68	2.86	1.76

a temperature denoted as T_a; both K and T_a depend on ρ. However, for $T < T_a$, K deviates from its constant value; this we attribute to the fact that taking $\psi = 1$ for $T < T_a$ is not valid. As argued above, the value of ψ is expected to decrease from its high-temperature value on cooling below T_a due to the increasing role of energy-driven processes which counter the escape of particles from shells. We have more to say about the constant K in Sec. V, where we calculate its value from the data of τ_α and show that it is indeed temperature independent and equal to the high-temperature value shown in Fig. 2.

Assuming that K remains constant at all temperatures and has value determined from high-temperature result plotted in Fig. 2 and listed in Table I, we determine $n^{(s)}(T)$ from Eq. (2.11). The known values of $n^{(s)}(T)$ allow us to find the temperature dependence of ψ from Eqs. (2.8)–(2.10). We plot $\psi(T)$ versus T in Fig. 3. We note that in all cases $\psi = 1$ for $T > T_a$ but decreases rather sharply for T less than T_a. Values of T_a for the three densities are given in Table I. In this table, we also list, for comparison's sake, values of "onset temperature" $T_{\rm onset}$ and mode-coupling temperatures T_{mc}. The $T_{\rm onset}$ is defined as the crossing temperature of pair and excess entropies [32] and T_{mc} is found by fitting data of τ_α in a power law form, $\tau_\alpha \propto (T - T_{mc})^{-\gamma}$, predicted by mode-coupling theory (MCT) [33]. According to MCT, T_{mc} is a temperature at which τ_α diverges, a prediction which is not observed. The temperature T_a falls in between $T_{\rm onset}$ and T_{mc} and seems to separate a high-temperature region, where slowdown of dynamics is slower, from a low-temperature region, where slowdown of dynamics is faster.

We now use value of ψ found at a given T and ρ in equations derived above to calculate different parts of $g_{\alpha\gamma}(r)$ and number of m and s particles. In Fig. 4, we plot $g_{\alpha\gamma}(r)$, $g^{(b)}_{\alpha\gamma}(r)$, and $g^{(s)}_{\alpha\gamma}(r)$ as a function of distance r for two temperatures $T = 0.45$ and 1.0 and the density $\rho = 1.2$ to show their temperature dependence. In Fig. 5, we explicitly show the spatial range of $g_{aa}(r)$, $g^{(f)}_{aa}(r) = g_{aa}(r) - g^{(b)}_{aa}(r)$, $g^{(m)}_{aa}(r) = g^{(b)}_{aa}(r) - g^{(s)}_{aa}(r)$, and $g^{(s)}_{aa}(r)$ for species a at $\rho = 1.2$ and $T = 0.45$. From the figure, one notes that while $g^{(s)}_{aa}(r)$ is confined in the first shell with length scale of the order of one particle diameter, $g^{(m)}_{aa}(r)$ extends to several shells with length scale of the order of several particle diameters. In this context, it is important to realize the role of ψ; as ψ decreases on cooling of the liquid, contributions to $g^{(s)}(r)$ start coming from other shells, extending the associated length scale. At a temperature where ψ becomes zero, all bonded particles become s particles and length scale of $g^{(s)}(r)$ will be same as that of $g(r) - 1$.

In Fig. 6, we plot number of total particles $[n_1^{(t)}(T)]$, bonded particles $[n_1^{(b)}(T)]$, m particles $[n_1^{(m)}(T)]$, and s particles $[n_1^{(s)}(T)]$ occupying the first shell as a function of inverse of the temperature $(1/T)$. We note that at high temperatures most particles are free, while few are m particles and very few are s particles. As the system is cooled, $n_1^{(m)}$ remains almost constant but $n_1^{(s)}$ increases slowly up to $T = T_a$. For $T < T_a$, $n_1^{(m)}(T)$ decreases while $n_1^{(s)}(T)$ increases with increasing rate at the cost of both free and m particles. As stated above, this rate will rapidly increase on further lowering of temperature, resulting in a rapid increase in the number of s particles. To have a precise nature of this increase, we need to have data of $g_{\alpha\gamma}(r)$ at lower temperatures.

III. CALCULATION OF THE POTENTIAL ENERGY BARRIER AND THE RELAXATION TIME

The potential energy barrier (activation energy) to relaxation, as stated above, is equal to the energy with which a particle is bonded with s particles. Thus,

$$\beta E^{(s)}(T,\rho) = 4\pi \sum_i \sum_\gamma x_\gamma \rho_\gamma \int_{r''_{il}}^{r''_{ih}} \left[\beta w^{(iu)}_{\alpha\gamma} - \psi(T) - \beta w^{(i)}_{\alpha\gamma}(r)\right] g^{(is)}_{\alpha\gamma}(r) r^2 dr, \tag{3.1}$$

where energy is measured from the effective barrier $\beta w^{(iu)}_{\alpha\gamma} - \psi(T)$. In Fig. 7, we plot values of $\beta E^{(s)}$ versus $1/T$ for different densities. In all the cases, we see sharp rise in $\beta E^{(s)}$ below T_a.

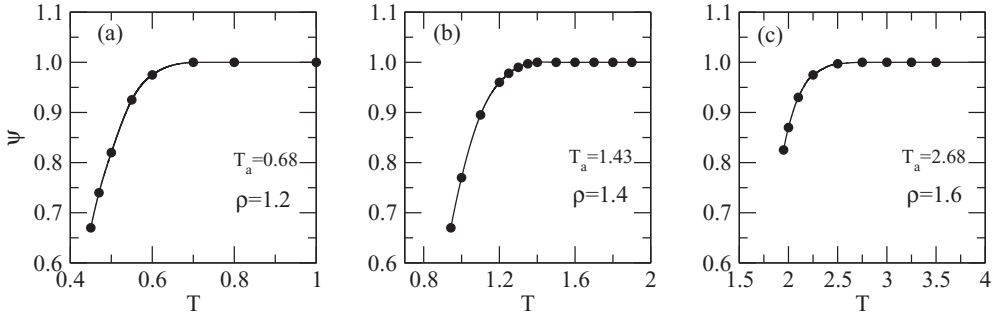

FIG. 3. Values of $\psi(T)$ as a function of temperature T at different densities. Symbols represent calculated values and curves are least-square fit.

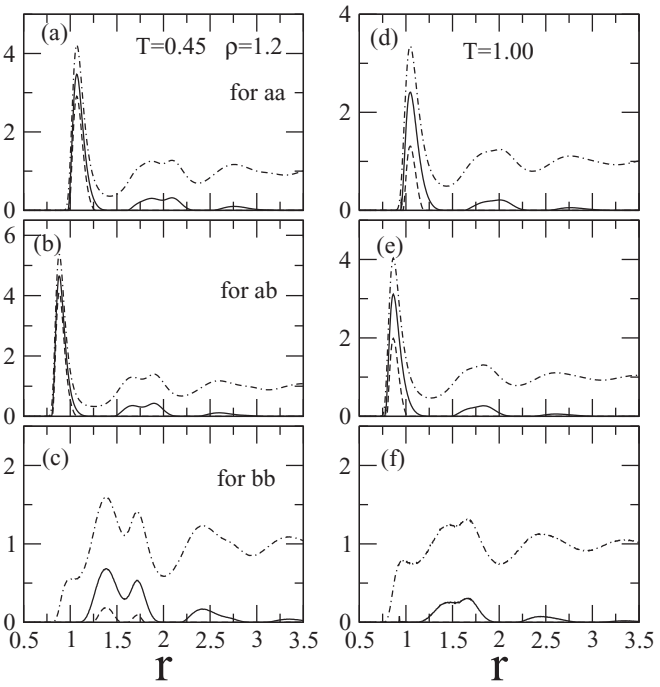

FIG. 4. Comparison of values of $g_{\alpha\gamma}(r)$ (dot-dashed line), $g^{(b)}_{\alpha\gamma}(r)$ (full line), and $g^{(s)}_{\alpha\gamma}(r)$ (dashed line) at two temperatures $T = 0.45$ and 1.0 and density $\rho = 1.2$.

The energy $\beta E^{(s)}$ can be considered as the activation energy in the Arrhenius law,

$$\tau_\alpha(T, \rho) = \tau_0 \exp[\beta E^{(s)}(T, \rho)]. \tag{3.2}$$

In Fig. 7, we compare calculated results with values found from computer simulations [31,34] for $\rho = 1.2$, 1.4, and 1.6. In all the cases, we find very good agreement between calculated and simulation values.

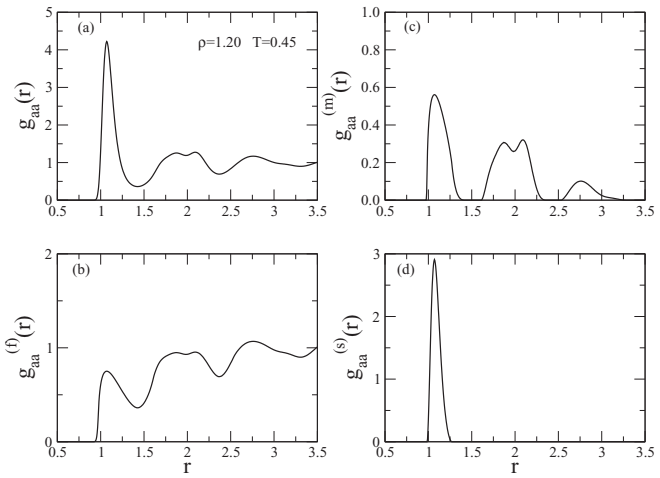

FIG. 5. Plot of $g_{aa}(r)$, $g^{(f)}_{aa}(r) = g_{aa}(r) - g^{(b)}_{aa}(r)$, $g^{(m)}_{aa}(r) = g^{(b)}_{aa}(r) - g^{(s)}_{aa}(r)$, and $g^{(s}_{aa})(r)$ as a function of r at $\rho = 1.2$ and $T = 0.45$.

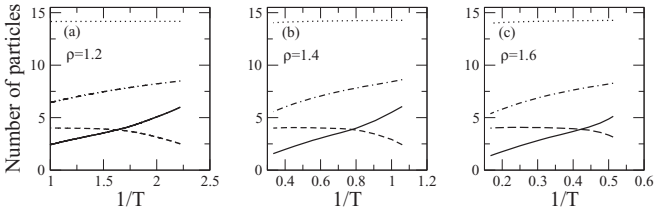

FIG. 6. Values of number of total $(n_1^{(t)})$ (dotted line), bonded $(n_1^{(b)})$ (dot-dashed line), metastable $(n_1^{(m)})$ (dashed line), and stable $(n_1^{(s)})$ (full line) particles occupying the first coordination shell as functions of $(1/T)$.

IV. THE TEMPERATURE T_a AND THE DENSITY SCALING

The density dependence of T_a is shown in Fig. 8. In the figure, full circles denote calculated values and the curve represents a fit with a power law form; $T_a = a_0\rho^\gamma$ with $a_0 = 0.287$ and $\gamma = 4.757$. If we renormalize the temperature T by T_a and plot values of $\psi(T)$ as a function of T/T_a, we find a very good collapse data of ψ at different densities as shown in Fig. 9(a). Similarly, when we plot $n^{(s)}(\rho, T)$, $\beta E^{(s)}(\rho, T)$, and $\tau_\alpha(\rho, T)/\tau_0$ as a function of T_a/T we find a very good collapse on master curves as shown in Figs. 9(b), 9(c), and 9(d), respectively.

The thermodynamic scaling through the variable ρ^γ/T, where γ is an intrinsic parameter stemming from the intermolecular interactions is found to be obeyed by a variety of liquids which may or may not be "strongly correlating liquids" [35–40]. The Lennard-Jones (L-J) liquid of Eq. (1.3) is a strongly correlating liquid [35–37]; it has strong correlations between their constant-volume equilibrium fluctuations of potential energy $U(t)$ and virial $W(t) = -1/3\sum_i \vec{r}_i \cdot \Delta_{\vec{r}_i} U(\vec{r}_1, \ldots, \vec{r}_N)$, where $U(t)$ is the total potential energy

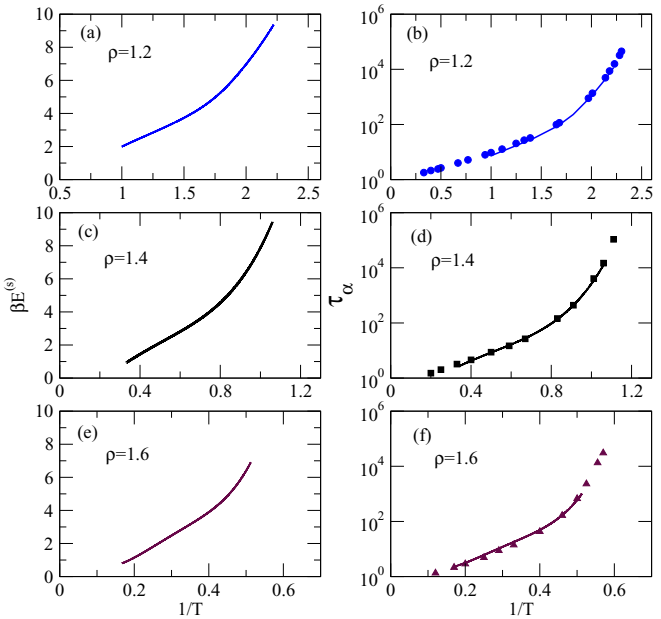

FIG. 7. Values of activation energy $\beta E^{(s)}$ for the relaxation and the relaxation time as a function of $1/T$ at three densities. Symbols denote simulation values and curves denote calculated values.

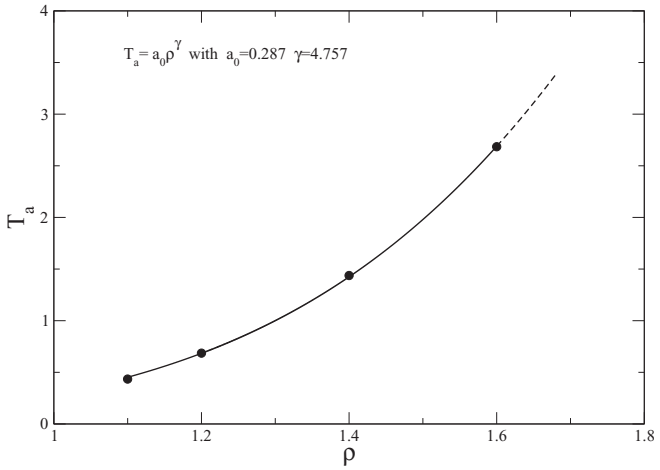

FIG. 8. Dependence of the temperature T_a on density ρ is shown. Full circles are calculated values and curve represents the fit $T_a = a_0\rho^{\gamma}$ with value of exponent $\gamma = 4.757$. The value of $T_a = 0.435$ at $\rho = 1.1$ was found from plotting τ_α values on the master curve.

at time t and $\vec{r}_i$ is the position of particle i at time t. The correlation is characterized by a single parameter Γ, defined by a linear fit through a scatter plot of time fluctuations of U and W. For the strongly correlating liquids, $\Gamma \simeq \gamma$. The parameter γ found from the slope of correlation plot as shown in Ref. [34] (see also Ref. [37]) has some arbitrariness; it varies between 4.56 and 5.03 for the model of Eq. (1.3). If we ignore this variation, the value can be considered to be in good agreement with the one found from the density dependence of T_a. This suggests that T_a is related to the "hidden scale invariance" [35–37] and is a result of strong WU correlations.

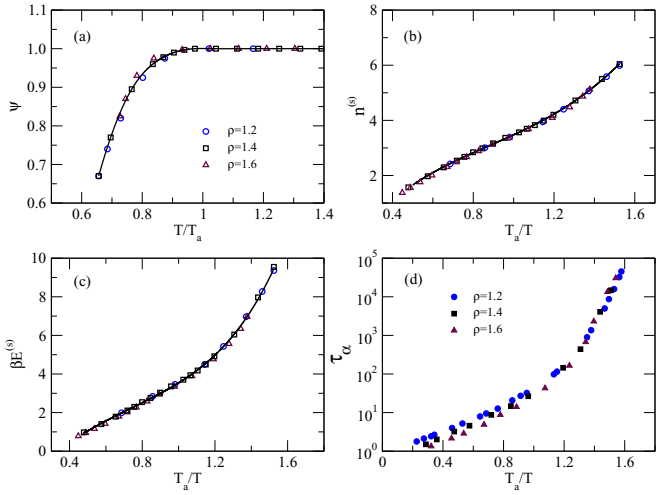

FIG. 9. Collapse of the data of ψ, $n^{(s)}$, $\beta E^{(s)}$ and τ_α at densities $\rho = 1.2$ to $\rho = 1.6$. In (a) ψ is plotted as a function of T/T_a whereas in (b), (c) and (d) values of $n^{(s)}$, $\beta E^{(s)}$ and τ_α are, respectively plotted as a function of T_a/T. In (a), (b) and (c) the (open) symbols represent calculated values and solid line determined from least square fitting is the master curve. In (d) the (filled) symbols represent values found from simulation [34]. This collapse of data on master curves shows that T_a is a characteristic temperature of supercooled liquids and intimately connected with fluctuations embedded in the system.

V. DISCUSSION

The theory described in this paper brings out several underlying features of the dynamics of fragile supercooled liquids. The local structural order, conceptualized as something which has to be a "very subtle and hidden to the pair correlation function," is shown to be the cooperatively reorganizing cluster (CRC) formed by a central particle with its neighbors of localized (s) particles and is determined from the radial distribution function, $g(r)$, by including momentum distribution in its definition. The particles in a CRC are distributed in coordination shells surrounding the central particle (see Fig. 1) and share the space with m particles. It is only at very low temperatures ($T \lesssim T_g$), where $\psi(T)$ becomes zero, all bonded particles become s particles, and CRC becomes a large and compact object. However, at high temperatures, where $\psi(T)$ is nonzero, CRC structure is not compact as the region is also occupied by m particles.

It may, however, be noted that a CRC is embedded at the center of a larger cluster of m particles. The cluster consisting of s and m particles, i.e., of $n^{(b)}$ particles, is large compared to CRC and is relatively compact (see Fig. 5). Since m particles are loosely bonded with the central particle, they move individually or in group of few particles on timescales much smaller than τ_α without affecting the structure of CRC. On the other hand, when a CRC reorganizes at timescales commensurable with τ_α, by moving its particles it may trigger reorganization of all particles of the cluster turning, it into a cluster of mobile particles. This picture seems to be in agreement with molecular dynamics simulations result [41], where α relaxation is found to be governed by rapid sporadic events characterized by emergence of relatively compact clusters of mobile particles. A similar result has also been found experimentally [42] from analysis of trajectories of several thousand suspended colloidal particles. Biroli *et al.* [43] developed inhomogeneous mode-coupling theory of dynamical heterogeneity and found that the geometrical structure carrying the dynamical correlations at timescales commensurable with that of the α relaxation is similar to the one found in Ref. [41]. It therefore seems that while the cluster that appears to take part in α relaxation is a cluster of bonded ($n^{(b)}$) particles which is large and relatively more compact than that of a CRC, it is the reorganization of particles of CRC that triggers the entire cluster to be mobile at timescales commensurable with τ_α; the energy involved in this is the energy of reorganization of a CRC.

The cooperativity of relaxation is defined in terms of the number of particles (or bonds) $n^{(s)}$ which are connected with the central particle in a CRC. For an event of relaxation to take place, these bonds have to rearrange irreversibly; the energy involved in this process is the effective activation energy $\beta E^{(s)}$ of relaxation. As the system is cooled, both the number $n^{(s)}$ and the energy of each bond increase; the combined effect makes $\beta E^{(s)}$ increase rapidly as temperature is lowered. A fit of (collapsed) data of $\beta E^{(s)}$ with a power law form $\beta E^{(s)} = b_0\{n^{(s)}\}^{\delta}$ with $b_0 = 0.415$ and $\delta = 1.73$ is shown in Fig. 10.

The parameter $\psi(T)$ which is introduced to measure the effect that the bath creates to stabilize the size of CRC gives insight into the processes underlying the slowdown of dynamics. The value of $\psi(T)$ takes a turn from its high-temperature value of 1 at $T = T_a$ and starts decreasing as T is lowered.

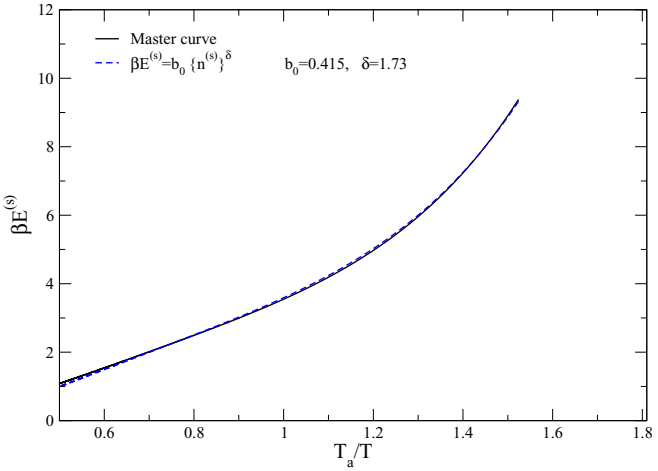

FIG. 10. Plot of the reduced activation energy $\beta E^{(s)}$ of relaxation as a function of T_a/T at densities $\rho = 1.2$, 1.4, and 1.6. The full line represents values found from the calculation and the dashed line represents a fit $\beta E^{(s)} = b_0\{n^{(s)}\}^{\delta}$, where $b_0 = 0.415$, $\delta = 1.73$, and $n^{(s)}$ is the number of bonds in a CRC [see Fig. 9(b)].

There is a crossover region (see Figs. 3 and 9) which separates the high-temperature behavior from the low-temperature behavior. Exactly the same behavior is seen (see Figs. 7 and 9) in τ_α; a crossover from the high-temperature ($T > T_a$) behavior to the low-temperature ($T < T_a$) behavior takes place in the same way as happens in the case of ψ. This is more clearly seen in Fig. 11, where we marked the two regions with straight lines to separate the crossover region. This brings forth the underlying cause for the temperature dependence of τ_α. The crossover region marks the change from the dominance of the entropy-driven process to the dominance of the energy-driven processes in the system on cooling.

Both ψ and T_a depend on details of the interparticle interactions. The value of temperature T_a is sensitive to the attraction in the potential; its value would increase upon increasing the attraction. Since the rate of slowdown of dynamics increases for $T < T_a$, the two systems with the same repulsion but a different attraction in the pair potential would show very different dynamics while $g(r)$ of the two systems may appear similar. This will be investigated in detail in our next publication.

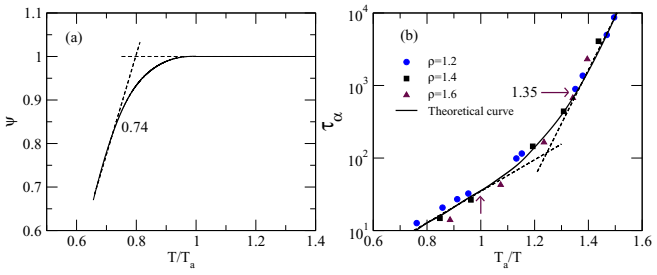

FIG. 11. Figures show the crossover region of $\psi(T)$ [in panel (a)] and τ_α [in panel (b)] from the high-temperature behavior to the low-temperature behavior on cooling. In both cases, the crossover region is in the range $0.74 \lesssim T/T_a \lesssim 1$. The straight lines (dashed line) are drawn to separate out the crossover region.

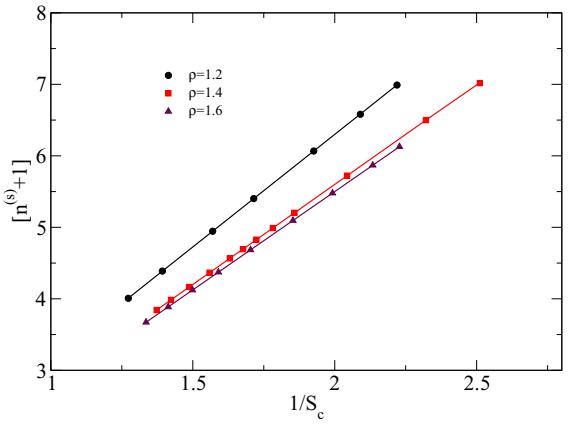

FIG. 12. Plot of number of particles $n^{(s)} + 1$ in a CRC vs $1/S_c$ at densities $\rho = 1.2$, 1.4, and 1.6. Lines show that the number $n^{(s)} + 1$ is inversely proportional to the configurational entropy S_c and the proportionality constant is temperature independent. Values of constants determined from the slope of these curves are 3.13, 2.81, and 2.75, respectively for $\rho = 1.2$, 1.4, and 1.6, which are nearly same as the one given in Table I.

We wish to emphasize that though Eq. (2.11) lacks theoretical rigour [17,44] it, as has been shown in Sec. II B, correctly describes the relationship between number of particles in a CRC and the configurational entropy. Here, we adopt a method different from the one described in Sec. II B and show that the number of particles in a CRC are inversely proportional to the configurational entropy and calculate the constant K. In particular, we now use data of τ_α/τ_0 determined from simulations in Eq. (3.2) to calculate $\beta E^{(s)}$ at different temperatures and then use these values in Eqs. (2.8)–(2.10) to calculate values of $\psi(T)$ and $n^{(s)}(T)$ [45]. The plot of $n^{(s)}(T) + 1$ versus $1/S_c(T)$ in Fig. 12 for the three densities show that $n^{(s)}(T) + 1$ is indeed inversely proportional to S_c and the proportionality constant K is temperature independent. Values of K found from the slope of curves of different densities are 3.13, 2.81, and 2.75, respectively for $\rho = 1.2$, 1.4, and 1.6, which are nearly same as the one given in Table I.

In summary, by including momentum distribution in the definition of the radial distribution function $g(r)$ and using the information of the configurational entropy S_c, we calculated the numbers of free, metastable, and stable particles distributed in coordination shells surrounding a central particle at different temperatures and densities. It is shown that in supercooled liquids the slowdown of dynamics is due to the emergence of cooperatively reorganizing clusters (CRCs) in which the central particle forms (nonchemical) "stable bonds" with neighboring stable particles. The CRC is embedded at the center of a larger and relatively compact cluster of $n^{(b)}$ particles. The number of bonds with which the central particle is bonded with neighbors defines the cooperativity of relaxation. For an event of relaxation to take place, these bonds have to reorganize irreversibly. Reorganization of bonds in a CRC triggers reorganization of all $n^{(b)}$ particles of the cluster, turning it into a cluster of mobile particles. The energy involved in this process is the effective activation energy $\beta E^{(s)}$ of relaxation. The number of bonds and the energy of each bond of the CRC increase in lowering the temperature and increasing the density. When $\beta E^{(s)}$ is substituted in the Arrhenius law,

a super-Arrhenius feature emerges. Results found for τ_α for the Kob-Anderson model system are in very good agreement with simulation results. The temperature dependence of τ_α is explained, in terms of the parameter $\psi(T)$ which measures the effect of fluctuations embedded in the bath on stabilizing the size of CRC.

ACKNOWLEDGMENTS

A.S. acknowledges support from a research fellowship from the Council of Scientific and Industrial Research, New Delhi, India. S.M.B. thanks SERB, India, for funding. We thank referees for bringing to our attention Refs. [38–43].

[1] C. A. Angell, Science **267**, 1924 (1995); P. G. Debenedetti and F. H. Stillinger, Nature (London) **410**, 259 (2001).
[2] F. Mallamace, C. Branca, C. Corsaro, N. Leone, J. Spooren, S. Chen, and H. E. Stanley, Proc. Natl. Acad. Sci. USA **107**, 22457 (2010).
[3] L. M. Martinez and C. A. Angell, Nature (London) **410**, 663 (2001).
[4] J. D. Stevenson, J. Schmalian, and P. G. Wolynes, Nat. Phys. **2**, 268 (2006).
[5] C. K. Mishra and R. Ganapathy, Phys. Rev. Lett. **114**, 198302 (2015).
[6] G. Adam and J. H. Gibbs, J. Chem. Phys. **43**, 139 (1965).
[7] T. R. Kirkpatrick, D. Thirumalai, and P. G. Wolynes, Phys. Rev. A **40**, 1045 (1989).
[8] M. D. Ediger and P. Harrowell, J. Chem. Phys. **137**, 080901 (2012).
[9] S. A. Kivelson and G. Tarjus, Nat. Mater. **7**, 831 (2008).
[10] G. Biroli and J. P. Garrahan, J. Chem. Phys. **138**, 012A301 (2013).
[11] L. Berthier and G. Biroli, Rev. Mod. Phys. **83**, 587 (2011).
[12] P. Crowther, F. Turci, and C. P. Royall, J. Chem. Phys. **143**, 044503 (2015).
[13] L. Berthier, P. Charbonneau, D. Coslovich, A. Ninarello, M. Ozawa, and S. Yaida, Proc. Natl. Acad. Sci. USA **114**, 11356 (2017).
[14] T. Kawasaki, T. Araki, and H. Tanaka, Phys. Rev. Lett. **99**, 215701 (2007).
[15] M. Mosayebi, E. DelGado, P. Ilg, and H. C. Ottinger, Phys. Rev. Lett. **104**, 205704 (2010).
[16] I. Tah, S. Sengupta, S. Sastry, C. Dasgupta, and S. Karmakar, Phys. Rev. Lett. **121**, 085703 (2018).
[17] J.-P. Bouchaud and G. Biroli, J. Chem. Phys. **121**, 7347 (2004).
[18] G. Biroli, J.-P. Bouchaud, A. Cavagna, T. S. Grigera, and P. Verrocchio, Nat. Phys. **4**, 771 (2008).
[19] A. Montanari and G. Semerjian, J. Stat. Phys. **125**, 23 (2006).
[20] G. M. Hocky, T. E. Markland, and D. R. Reichman, Phys. Rev. Lett. **108**, 225506 (2012).
[21] C. Cammarota and G. Biroli, EPL **98**, 36005 (2012).
[22] J. Kurchan and D. Levine, J. Phys. A **44**, 035001 (2011).
[23] F. Sausset and D. Levine, Phys. Rev. Lett. **107**, 045501 (2011).
[24] X. Xia and P. G. Wolynes, Proc. Natl. Acad. Sci. USA **97**, 2990 (2000).
[25] V. Lubchenko and P. G. Wolynes, J. Chem. Phys. **119**, 9088 (2003).
[26] A. Singh and Y. Singh, Phys. Rev. E **99**, 030101(R) (2019).
[27] W. Kob and H. C. Andersen, Phys. Rev. Lett. **73**, 1376 (1994).
[28] J. P. Hansen and I. R. McDonald, *Theory of Simple Liquids*, 3rd ed. (Academic Press, Burlington, VT, 2006).
[29] S. Sastry, Phys. Rev. Lett. **85**, 590 (2000); Nature (London) **409**, 164 (2001).
[30] L. Berthier, M. Ozawa, and C. Scalliet, J. Chem. Phys. **150**, 160902 (2019).
[31] A. Banerjee, M. K. Nandi, S. Sastry, and S. M. Bhattacharyya, J. Chem. Phys. **145**, 034502 (2016).
[32] A. Banerjee, M. K. Nandi, S. Sastry, and S. M. Bhattacharyya, J. Chem. Phys. **147**, 024504 (2017).
[33] W. Götze, *Complex Dynamics of Glass-Forming Liquids: A Mode-Coupling Theory* (Oxford University Press, Oxford, UK, 2008).
[34] L. Berthier and G. Tarjus, Phys. Rev. Lett. **103**, 170601 (2009); J. Chem. Phys. **134**, 214503 (2011).
[35] N. P. Bailey, U. R. Pedersen, N. Gnan, T. B. Schrøder, and J. C. Dyre, J. Chem. Phys. **129**, 184507 (2008); **130**, 039902 (2009).
[36] T. B. Schrøder, N. Gnan, U. R. Pedersen, N. P. Bailey, and J. C. Dyre, J. Chem. Phys. **134**, 164505 (2011).
[37] A. Grzybowski, K. Koperwas, and M. Paluch, Phys. Rev. E **86**, 031501 (2012).
[38] C. M. Roland, S. Hensel-Bielowka, M. Paluch, and R. Casalini, Rep. Prog. Phys. **68**, 1405 (2005).
[39] F. Puosi, O. Chulkin, S. Bernini, S. Capaccioli, and D. Leporini, J. Chem. Phys. **145**, 234904 (2016).
[40] Y.-C. Hu, B.-S. Shang, P.-F. Guan, Y. Yang, H.-Y. Bai, and W.-H. Wang, J. Chem. Phys. **145**, 104503 (2016).
[41] G. A. Appignanesi, J. A. Rodriguez Fris, R. A. Montani, and W. Kob, Phys. Rev. Lett. **96**, 057801 (2006).
[42] J. A. R. Fris, G. A. Appignanesi, and E. R. Weeks, Phys. Rev. Lett. **107**, 065704 (2011).
[43] G. Biroli, J.-P. Bouchaud, K. Miyazaki, and D. R. Reichman, Phys. Rev. Lett. **97**, 195701 (2006).
[44] A. Cavagna, Phys. Reports **476**, 51 (2009).
[45] A. Singh and Y. Singh, arXiv:1909.02734.